Int. J. Therm. Sci. (1999) 38, 442-451

Theoretical analysis of environmental and energetic performance of very high temperature turbo-jet engines

Thierry Godin[a*], Simon Harvey[b**], Pascal Stouffs[b***]

[a] *École des mines de Nantes, 4, rue Alfred Kastler, BP 20722, 44307 Nantes cedex 3, France*
[b] *Isitem, La Chantrerie, BP 90604, 44306 Nantes cedex 3, France*

(Received 4 May 1998, accepted after revision 20 October 1998)

Abstract — Current progress in gas turbine performance is achieved mainly by increasing the turbine inlet temperature. State-of-the-art military aircraft gas turbines operate with turbine inlet temperatures exceeding 2 000 K, and future development plans call for even higher temperature levels. At such high temperatures, the hot combustion gases can no longer be considered as chemically inert, and it becomes important to account for the chemically reactive nature of the expanding flow. In this paper, the authors present a one-dimensional model of the chemically reactive flow through the first turbine stage of an aircraft turbo-jet engine. The model is used to study the impact of chemical reactivity on pollutant emission characteristics and engines performance (i.e. overall efficiency and specific thrust). Three different casess are considered: sea-level static operation (take-off), commercial aircraft in subsonic cruising at 10 000 m altitude, and military aircraft in supersonic flight at 20 000 m altitude. The results of this study show, for instance, that the production of environmental pollutants in the turbine as a result of chemical reactivity is particularly significant for turbo-jets operating at subsonic cruise velocities. Moreover, in both flight conditions considered, the increase of operating temperature decreases the overall efficiency. © Elsevier, Paris.

reactive flow / turbo-jet / pollutant emission / high temperature gas turbine / aircraft engine performance

Résumé — Analyse théorique des performances environnementales et énergétiques des turboréacteurs à très haute température. La température des gaz à l'entrée de la turbine des turboréacteurs aéronautiques militaires de dernière génération dépasse actuellement 2 000 K, et différents projets prévoient des fonctionnements à température encore plus haute. À ces niveaux de température, les gaz de combustion ne peuvent plus être considérés comme inertes. Il devient important de tenir compte de la réactivité chimique du fluide qui subit la détente. Dans cet article, les auteurs présentent un modèle unidimensionnel de l'écoulement réactif dans le premier étage de la turbine d'un turboréacteur aéronautique. Ce modèle est utilisé pour étudier l'impact de la réactivité chimique sur les émissions polluantes et sur les performances des moteurs (rendement global, poussée spécifique). Trois cas différents sont considérés : point fixe, avion commercial en croisière subsonique à 10 000 m d'altitude et avion militaire en vol supersonique à 20 000 m d'altitude. Les résultats de cette étude montrent entre autres que la production de polluants dans la turbine par suite de la réactivité chimique est particulièrement importante dans le cas des turboréacteurs en vitesse de croisière subsonique. En outre, pour les deux conditions de vol considérées, une augmentation de la température d'entrée des gaz dans la turbine conduit à une diminution du rendement global. © Elsevier, Paris.

écoulement réactif / turboréacteur / émission de polluants / turbine à gaz à haute température / performances des moteurs aéronautiques

Nomenclature

A	nozzle section	m^2
c_p	specific heat	$J \cdot kg^{-1} \cdot K^{-1}$
F	specific thrust	$N \cdot s \cdot kg^{-1}$
h	specific mass enthalpy	$J \cdot kg^{-1}$
h_f°	molar formation enthalpy	$J \cdot mol^{-1}$
ΔH_r°	heat of reaction	$J \cdot mol^{-1}$
Δh_{st}	absolute enthalpy drop in the stage	$J \cdot kg^{-1}$
LHV	lower heating value	$J \cdot kg^{-1}$
M	molar mass	$kg \cdot mol^{-1}$
$\dot{m}$	mass flux	$kg \cdot s^{-1}$
n_t	total mole number	mol
p	pressure	Pa

* Present address: Ensam, 2, bd du Ronceray, BP 3525, 49035 Angers cedex, France.

** Present address: Chalmers University of Technology, Inst. for Varmeteknik och Maskinlara, Kemivagen, 4. 412 96 Göteborg, Sweden.

*** Correspondence and reprints.
pascal.stouffs@isitem.univ-nantes.fr

q	chemical heat released in the stage	$J \cdot kg^{-1}$
$\dot{Q}$	energy supply rate	W
T	temperature	K
TIT	turbine inlet temperature	K
v	absolute gas velocity	$m \cdot s^{-1}$
v_0	cruise velocity	$m \cdot s^{-1}$
w_5	nozzle exit relative gas velocity	$m \cdot s^{-1}$
$\mathcal{W}$	specific work	$J \cdot kg^{-1}$
x_i	molar fraction	$mol_i \cdot mol^{-1}$
y_i	mass fraction	$kg_i \cdot kg^{-1}$
z	shaft axis	m

Greek Symbols

η_{chr}	chemical heat release efficiency
η_{pro}	propulsion efficiency
$\eta_{p,c}$	polytropic compression efficiency
$\eta_{p,i}$	polytropic intake efficiency
$\eta_{p,t}$	polytropic turbine efficiency
$\eta_{p,n}$	polytropic nozzle efficiency
η_{th}	thermal efficiency
η_o	overall efficiency
Λ	degree of reaction
ρ	density ($kg \cdot m^{-3}$)
Φ	equivalence ratio
$\dot{\omega}_i$	chemical species production rate ($mol_i \cdot m^{-3} \cdot s^{-1}$)

Subscripts

co	relative to a complete oxidation
f	relative to a chemically inert flow

1. INTRODUCTION

In order to improve thermal efficiency, gas turbines have evolved considerably in recent years with respect to their maximum working fluid temperatures and pressures. State-of-the-art military aircraft gas turbines operate with turbine inlet temperatures exceeding 2 000 K. Ambitious research programs are investigating turbo-jet engine operation with Turbine Inlet Temperatures (TIT) close to the stoichiometric flame temperature within the foreseeable future [1, 2].

Current design procedures assume that the combustion reaction process proceeds to completion in the combustion chamber, and that the combustion products can be considered as chemically inert in the downstream sections of the engine. At high temperature levels, this assumption is no longer valid, and the combustion gases contain dissociated, incompletely oxidized species. This has two effects on engine operation. First of all, the presence of incompletely oxidized combustion products at the combustor exit implies that the full fuel heating value (LHV) has not been released as heat. A fraction of LHV thus remains as potential chemical energy. The second effect results from the chemically reactive nature of the hot combustion gases, whereby the final reaction steps of the combustion process continue to occur within the turbine itself. A further fraction of the fuel heating value is thus released during the hot gas expansion. However, as a result of the rapidly changing flow conditions in the turbine, the combustion reactions do not proceed to completion in the turbine stage. At the turbine outlet, the cooled expanded gases therefore still contain dissociated species, resulting in significant levels of pollutant emissions. Furthermore, the fraction of LHV not released in the combustor is therefore not fully recovered in the turbine.

Given the fast changes in pressure and temperature during the expansion, the above-mentioned chemical reactions are far from equilibrium. A coupled analysis with respect to both aerodynamics and thermo-chemistry is thus necessary to study the flow characteristics in this part of the engine.

In a previous paper [3], the authors investigated the influence of the chemical reactivity on the expansion characteristics in a stationary gas turbine using a one-dimensional flow model. This preliminary investigation showed clearly that at high turbine inlet temperatures, incompletely oxidized species are present at the combustor outlet. As the expansion proceeds, part of the incompletely oxidized species (mainly CO and H_2) recombine with oxygen, forming CO_2 and H_2O and releasing a further amount of heat. This heat release affects the expansion characteristics and is mainly observed in the first stage of the turbine. The study concluded that chemical reactivity has a significant impact on turbine flow characteristics for TITs above 2 000 K.

Currently, the highest TITs are observed for aircraft engines. Thus, the one-dimensional model of the reactive flow was further developed and applied to a simple turbo-jet engine [4]. The first part of this paper presents results from the one-dimensional model showing the impact of chemically reactive flow in the turbine on pollutant emission characteristics. In the second part of the paper a cycle analysis is developed in order to study the influence of very high TIT on engine performance (i.e., overall efficiency and specific thrust). For both parts of the study three typical aircraft operating conditions are considered: sea-level static operation (take-off), commercial aircraft in subsonic flight (10 000 m, $Mach = 0.86$) and military aircraft in supersonic flight (20 000 m, $Mach = 2.5$).

2. DESCRIPTION OF THE 1-D FLOW MODEL

Figure 1 shows the main components of a simple turbo-jet engine [5]. The assumptions and equations used to model the different sections of the engine are

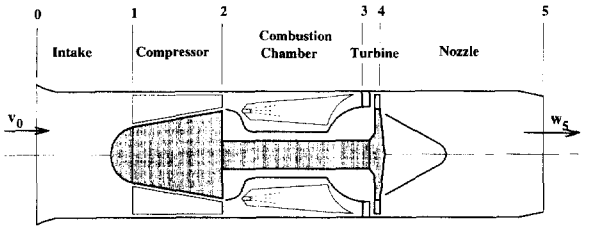

Figure 1. Simple turbo-jet engine.

briefly summarized below. The reader is referred to previous papers [3, 4, 6] for a more complete description. The working fluid is assumed to behave like an ideal gas throughout the engine.

2.1. Engine intake

The ambient temperature and pressure values are taken from the *International Standard Atmosphere* tables. Because of the significant effect of forward speed the intake is modeled as a separate component. The intake is considered as an adiabatic duct. Since there is no heat or work transfer, the stagnation temperature is constant although there will be a loss of stagnation pressure due to friction and shock waves for supersonic flight conditions.

For commercial aircraft at subsonic speeds, diffusion in the inlet duct is modeled by considering the intake polytropic efficiency $\eta_{p,i}$, with $\eta_{p,i} = 0.95$.

For military aircraft at supersonic speeds, the compressor inlet pressure results from the pressure rise across a system of shock waves at the inlet followed by that due to subsonic diffusion in the remainder of the duct [7]. For the case considered (20 000 m, $Mach = 2.5$) we assume a system of shock waves including an oblique shock wave followed by a normal shock wave [4].

2.2. Compressor

The compressor provides the work necessary to finish compressing the inlet air to the specified combustor pressure. The compression is modeled using the compressor polytropic efficiency $\eta_{p,c}$, with $\eta_{p,c} = 0.89$.

2.3. Combustion chamber

Pressure drops in the combustor are neglected. The burnt-gas mixture composition at the combustor exit is computed for specified pressure and temperature (TIT) conditions, assuming adiabatic reactor behavior. The gas mixture at the exit of the combustion system can be characterized by the following hypotheses:

- the gas mixture entering the nozzle guide vane is free of hydrocarbon molecules;
- the mixture is assumed to be at chemical equilibrium, with the exception of the NO species;
- the gas mixture contains the following 11 species: CO_2, CO, H_2O, H_2, H, OH, O_2, O, N_2, N and NO.

The jet-fuel considered in this study is kerosene with physical properties similar to $C_{12}H_{26}$. The fuel is assumed to enter the combustor at the operating pressure and at 400 K. The molar composition at equilibrium is easily computed using STANJAN [8]. The combustion equation can be written as follows:

$$\begin{aligned}\Phi\, C_{12}H_{26} + \frac{37}{2}(O_2 + 3.76\, N_2) \\ \rightarrow n_t\,(x_{CO_2}\, CO_2 + x_{CO}\, CO + x_{H_2O}\, H_2O \\ + x_{OH}\, OH + x_{O_2}\, O_2 + x_{H_2}\, H_2 + x_O O \\ + x_H\, H + x_N\, N + x_{N_2}\, N_2 + x_{NO}\, NO)\end{aligned} \quad (1)$$

where Φ denotes the equivalence ratio, and n_t the total number of moles in the combustion products, with $n_t = \dfrac{139.12}{2\,x_{N_2} + x_{NO} + x_N}$.

In practice, NO concentrations at the combustion chamber outlet are considerably lower than those indicated by equilibrium calculations. According to emission regulations described in [9], the NO concentration is set equal to 11.3 $g \cdot kg_{fuel}^{-1}$ for all simulation cases. CO concentrations are also significantly different in practice compared to the equilibrium value computed at the mean combustor outlet temperature. This is due to the temperature fluctuations in the combustor flow, caused by the fluctuations of equivalence ratio. However, it is reasonable to assume that the CO concentrations are at equilibrium on a local scale at the combustor outlet. The simulation methods proposed in this paper can then be applied individually to the different "pockets" of combustor outlet gases, provided a reasonable temperature distribution is assumed at the combustor outlet. Further discussion of this point together with accompanying results may be found in a previous paper [3].

2.4. Turbine first stage flow equations

The intent of the present paper is to provide insight about the interaction between the working fluid chemical reactivity and other flow characteristics. The model thus considers one-dimensional stationary flow, the spatial dimension considered being the shaft axis z. The model is further simplified by assuming adiabatic and frictionless flow. Due to the current high turbine efficiency it is thought that the approximation level induced by this latter assumption is lower than the one due to the choice of a one-dimensional pressure specified flow model.

Because of the fast temperature decrease in the turbine, the fluid chemical evolution is mainly located

at the expansion start [3]. Thus this model is applied to the turbine first stage only.

Steady-state, chemically reactive, adiabatic, frictionless one-dimensional flow in the turbine first stage can be described by the following equations expressing conservation of mass, momentum and energy, and chemical species balances (one equation per chemical species), respectively:

$$\mathrm{d}(\rho A v) = 0 \tag{2}$$

$$\rho v \frac{\mathrm{d}v}{\mathrm{d}z} + \frac{\mathrm{d}p}{\mathrm{d}z} = 0 \ \text{(stator)}; \quad = \rho \frac{\mathrm{d}\mathcal{W}}{\mathrm{d}z} \ \text{(rotor)} \tag{3}$$

$$\frac{\mathrm{d}h}{\mathrm{d}z} + v \frac{\mathrm{d}v}{\mathrm{d}z} = 0 \ \text{(stator)}; \quad = \frac{\mathrm{d}\mathcal{W}}{\mathrm{d}z} \ \text{(rotor)} \tag{4}$$

$$\rho v \frac{\mathrm{d}y_i}{\mathrm{d}z} = \dot{\omega}_i M_i \tag{5}$$

$\mathcal{W}$ refers to the specific work produced by one unit mass of fluid as it expands in the rotor wheel. In order to evaluate the right-hand side terms in equations (3) and (4), we introduce the assumption that the local *degree of reaction* Λ is constant throughout the rotor wheel. This leads to:

$$\frac{\mathrm{d}\mathcal{W}}{\mathrm{d}z} = \frac{1}{\Lambda} \frac{\mathrm{d}h}{\mathrm{d}z} \tag{6}$$

Flow through the nozzle followed by the rotor wheel may now be modeled by coupling equations (2) through (6) with appropriate equations describing the chemical reaction rates (see below). The resulting set of ordinary differential equations is then solved using an ODE solver.

The fluid undergoes very rapidly changing temperature and pressure conditions while expanding through the turbine. To correctly account for the resulting fluid composition variations, a detailed chemical reaction scheme is considered. The reaction scheme is a reduced scheme based on a complete reaction scheme proposed by Miller and Bowman [10] for combustion of methane. The complete scheme was reduced for computational simplicity. The reaction scheme proposed yields essentially identical results compared to a reaction scheme with 19 reactions involving the 11 chemical species listed in a previous paragraph. Details of the simulation results undertaken in order to reduce the number of reactions considered may be found in reference [11]. The reaction scheme is shown in *table I*.

The reaction kinetics for the forward reactions are described using *Arrhenius* expressions for the reaction rates, with rate constants taken from [10]. The reverse reaction rates are calculated from the reaction equilibrium constants. All reaction rates are computed using the CHEMKIN-II package [12].

The simulation proceeds by imposing a half-period sinusoidal pressure profile on the fluid. The turbine inlet *Mach* number is set equal to 0.2 in all cases. The stator outlet pressure is chosen for transonic ($Mach = 1.1$) operation. Subsonic operation is assumed in the rotor. The choice of the outlet rotor pressure results from a detailed analysis of the flow velocity vector diagram [3]. Conservation of the flow axial velocity component is assumed, and purely axial flow at the rotor outlet is imposed. The rotor velocity is set such that the degree of reaction is equal to the chosen value 0.3. This value is representative of current machine design practice.

TABLE I
Reaction scheme.

	Reaction mechanism		
1	$CO + OH$	$\rightleftharpoons$	$CO_2 + H$
2	$CO + O + M$	$\rightleftharpoons$	$CO_2 + M$
3	$O + OH$	$\rightleftharpoons$	$O_2 + H$
4	$O + H_2$	$\rightleftharpoons$	$OH + H$
5	$H + H + M$	$\rightleftharpoons$	$H_2 + M$
6	$H + OH + M$	$\rightleftharpoons$	$H_2O + M$
7	$O + O + M$	$\rightleftharpoons$	$O_2 + M$
8	$N + NO$	$\rightleftharpoons$	$O + N_2$
9	$N + O_2$	$\rightleftharpoons$	$NO + O$

2.5. Operating conditions

Since dissociation and recombination reactions occur only at very high temperatures, simulations were run for two TIT values: 2 100 K and 2 400 K. 2 100 K is representative of TIT levels attained in state-of-the-art high performance military jet engines. As discussed in the introductory section of the paper, a number of ambitious research programs are currently investigating the possibility of near-stoichiometric engine operation. Thus, simulations were run with a TIT of 2 400 K, which is close to stoichiometric conditions for most flight conditions considered. *Table II* lists the turbine inlet conditions that were chosen for the present study.

The operating temperature $TIT = 2\,400$ K cannot be reached at sea-level static conditions with a compression ratio set to 5. In this particular case the compression ratio begins at 6.

TABLE II
Simulation conditions.

Aircraft	Altitude	*Mach*	Compression ratio
	sea-level	0	5–50
commercial	10 000 m	0.86	10–50
military	20 000 m	2.5	5–25

3. RESULTS OF THE 1-D FLOW MODEL

3.1. Pollutant emissions

Figure 2 shows NO mole fraction profiles. We recall that NO composition at the turbine inlet is set equal to 11.3 $g \cdot kg_{fuel}^{-1}$. At $TIT = 2\,100$ K, the production of thermal NO within the stage is negligible, whereas at 2 400 K we observe a significant production of NO. The effects of compression ratio are clear: for all flight conditions considered, the NO mole fraction decreases with compression ratio, whereas the NO production rate increases. The effect of altitude is less clear: for stationary sea level operation, we observe high NO mole fractions, and high levels of NO production within the turbine. At commercial flight altitude, the NO production within the turbine is less pronounced. At high altitude, the NO mole fractions are lower, but the production within the turbine is significantly greater than for operation at 10 000 m.

Figure 3 shows CO mole fraction profiles. Unlike the NO mole fraction profiles, we note a similar behavior at both TIT levels considered. However, the scales of the two parts of the figure are very different. Thus, at 2 100 K, the absolute difference between CO emissions

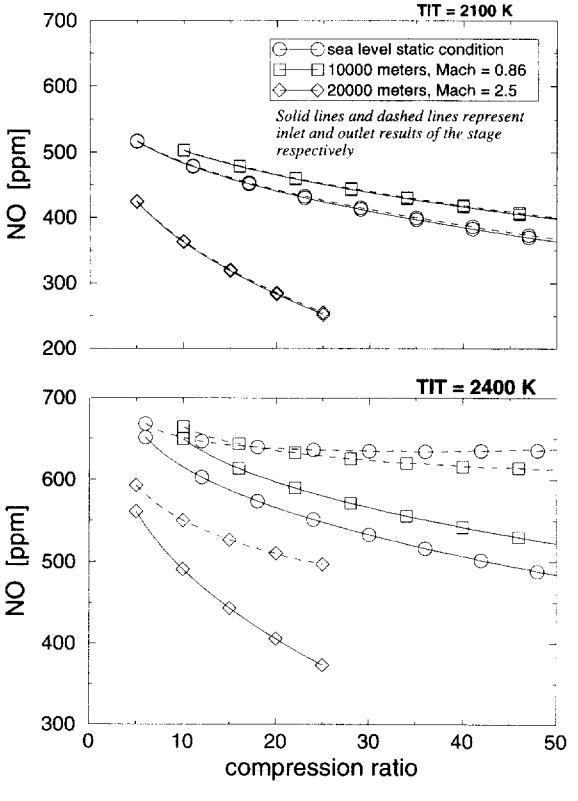

Figure 2. NO mole fraction vs. compression ratio.

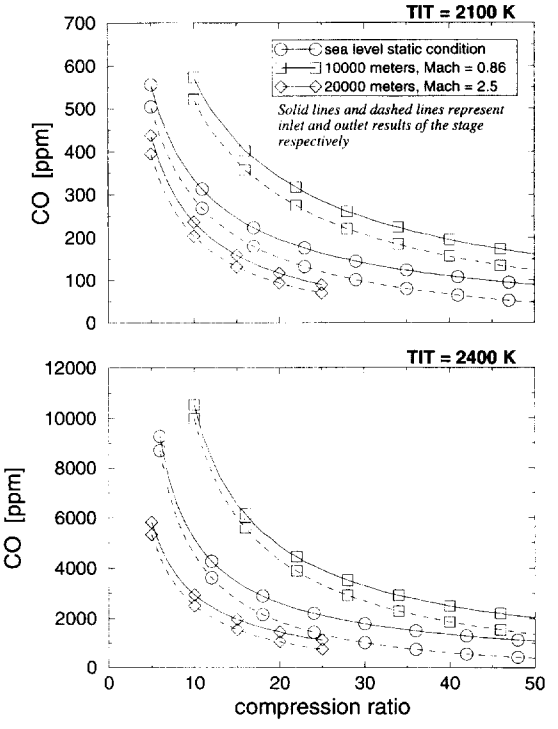

Figure 3. CO mole fraction vs. compression ratio.

at the combustor outlet and at the engine outlet is much smaller than at 2 400 K. We recall that CO is assumed to be at equilibrium at the turbine inlet, which explains the high values noted at the turbine inlet for $TIT = 2\,400$ K. For low compression ratios, the high CO composition values result from the low pressure levels which favor molecular dissociation of CO_2 and from the combustor overall equivalence ratio Φ which is close to unity, implying near stoichiometric combustor operation.

Note that the CO recombination reaction is the major internal heat source for the expanding gas stream, and this reaction is responsible for most of the temperature increase compared to a non reactive flow. During the expansion process, the rapid decrease of pressure and temperature favors the recombination of CO to form CO_2. However, this recombination process is governed by reaction kinetics and the exit CO composition is far from equilibrium. Thus, we observe a large amount of CO at the nozzle exit.

Figure 4 shows profiles of the chemical heat release efficiency η_{chr}. This efficiency is a measure of the fraction of the fuel heating value which has not been released due to the presence of dissociated and partially oxidized species. We define this efficiency as follows:

$$\eta_{chr} = \frac{\sum_i n_t \, x_i \, h^\circ_{f,i} - \Phi h^\circ_{f,C_{12}H_{26}}}{\Phi \Delta H^\circ_{r,C_{12}H_{26}}} \qquad (7)$$

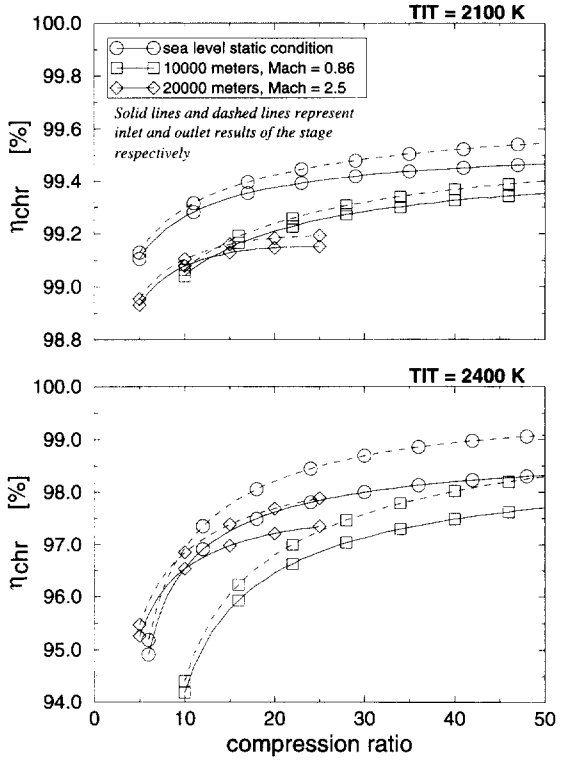

Figure 4. η_{chr} vs. compression ratio.

η_{chr} can thus be computed at any location in the expansion path. At the combustor outlet, the definition of η_{chr} is similar to that of the combustion efficiency, as defined in reference [9].

We note that at the turbine inlet η_{chr} is well below 100 % in all cases. At supersonic speed, for example, η_{chr} only reaches 95 % at 2 400 K for low compression ratios. Thus, 5 % of the fuel heating value remains unreleased. During the expansion process, the recombination of dissociated species (mainly CO and H_2) leads to an increase of η_{chr}. However, the recombination reactions are not sufficient to recover all the fuel heating value. We also observe that the recombination reactions are more active at sea-level static conditions than in flight conditions.

3.2. Effect of altitude and cruise velocity

In this section, we compare emissions characteristics of a given jet-engine operating at take-off with those of an engine in flight conditions, based on a visual analysis of the curves in *figures 2* and *3*. We consider the high temperature case, i.e. $TIT = 2\,400$ K.

Let us first consider a jet engine operating at a fixed compression ratio. At subsonic velocities, we observe (*figure 3*) that the CO composition at the stage inlet is approximately twice that observed at the stage inlet for sea level static operation. At the stage outlet, the amount of CO is reduced as a result of recombination reactions, but the CO composition remains higher than that observed at the combustor outlet for stationary operation. Thus, subsonic cruising operation with a fixed compression ratio leads to significantly increased CO emissions compared to sea level stationary operation. For the NO species (*figure 2*), we observe that the outlet NO levels observed are very close for a given compression ratio. The amount of NO produced within the turbine stage itself is however greater for the stationary case. Comparing stationary and supersonic operating conditions, we observe less CO and NO for flight operating conditions. The CO level decrease in supersonic flight compared to sea level static operation could seem surprising with regards to the absolute pressure reduction. Actually the CO decrease is due to a lower equivalence ratio Φ. Indeed in supersonic flight conditions the entering fluid undergoes an important temperature rise due to dynamic compression. So less fuel is needed in order to attain the prescribed TIT.

In practice however, jet engine compression ratios usually decrease with altitude in order to increase the specific thrust. For subsonic operation, this results in a further slight increase in outlet NO composition, and to a significant increase in outlet CO composition. For supersonic operation, decreasing the compression ratio increases the outlet emissions levels compared to levels encountered with the compression ratio considered for stationary operation. However, unless the compression ratio decreases significantly, the outlet levels of CO and NO are generally lower than those observed for stationary operation.

Thus, we observe that the chemically reactive nature of the expanding gas stream has a strong effect on the production of environmental pollutants. The effect is particularly pronounced for turbo-jet engine operation at subsonic cruise velocities.

3.3. Heat release in turbine stage

As we discussed previously, heat is released in the turbine stage, and thus the temperature decreases less rapidly than if non reactive flow is assumed. The computed temperature difference at the stage outlet between the two types of flow is denoted ΔT. *Figure 5* shows that ΔT increases with compression ratio. One of the key reasons is that pressure favors the recombination reactions, thus more heat is released at high pressure. For $TIT = 2\,400$ K, the temperature difference is significant and exceeds 10 K at sea-level static conditions. As we discussed previously, we also note that the difference in temperature is less important for flight conditions due to a reduced rate of recombination reactions.

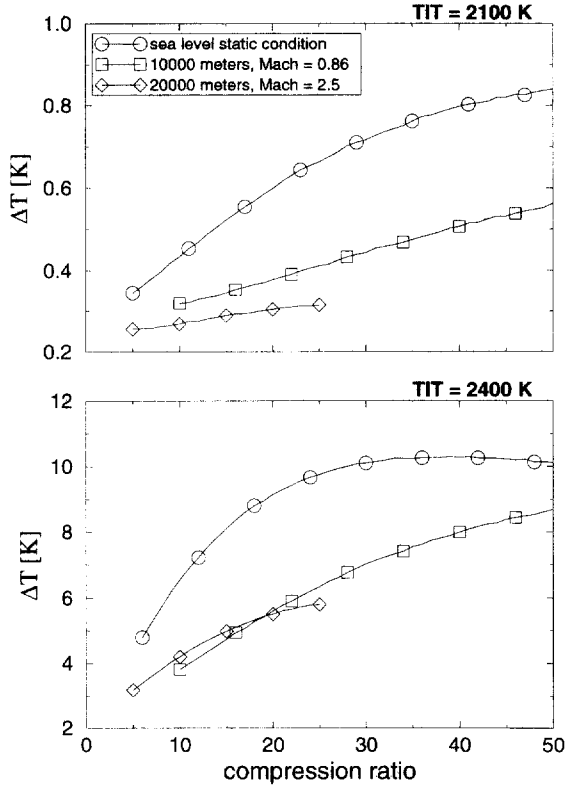

Figure 5. ΔT vs. compression ratio.

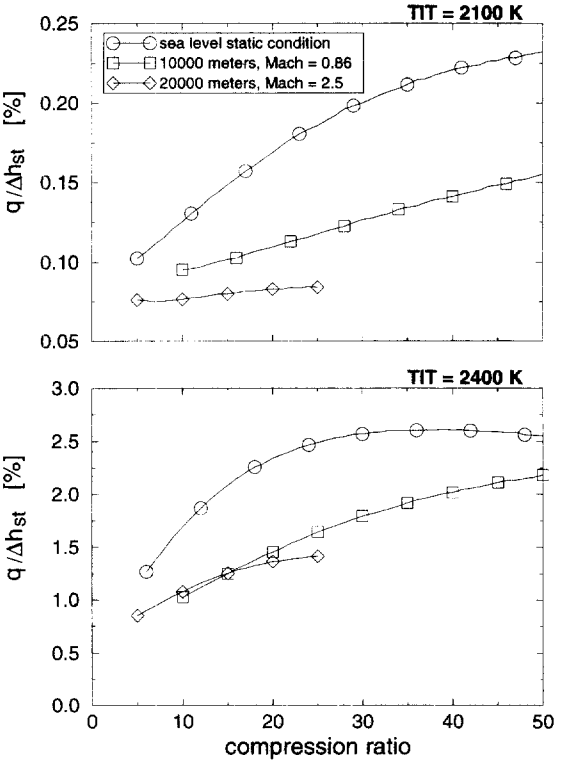

Figure 6. $q/\Delta h_{st}$ ratio vs. compression ratio.

Figure 6 shows $q/\Delta h_{st}$ ratio profiles where q is the measure of the heat released by recombination reactions in the turbine stage and Δh_{st} represents the absolute enthalpy drop. Referring to *figure 7*, q and Δh_{st} are defined as follows:

$$q = \left(\frac{1}{M}\sum_i n_t\, x_i\, h^\circ_{f,i}\right)_3 - \left(\frac{1}{M}\sum_i n_t\, x_i\, h^\circ_{f,i}\right)_4$$

where M denotes the gas mix molar mass, and

$$\Delta h_{st} = h_4 - h_3$$

The profiles shown in *figure 6* are very similar to those obtained in *figure 5*. At $TIT = 2\,100$ K, the chemical heat released q represents a very low fraction of the energy recovered in the stage (< 0.25 %). Conversely, at $TIT = 2\,400$ K, q levels are significant (over 2.5 % of Δh_{st} for sea-level static operation with high compression ratios). With such considerable differences observed within the expansion turbine itself at high temperatures, it appears clear that the thermodynamic characteristics of the gas stream are modified. The purpose of the following sections is to investigate how the chemical reactivity influences the performance characteristics of the whole engine.

4. ANALYSIS OF ENGINE PERFORMANCE

In this section we present a cycle analysis which has been developed in order to study the influence of chemical reactivity on performance characteristics of a turbo-jet engine. Full details of this analysis may be found in reference [13]. The following hypotheses (air standard cycle [5]) were retained for this analysis:

- the reacting gas mixture is assumed to be a perfect gas;
- the mass flow $\dot{m}$ is constant;
- the pressure losses in the combustor and pipes are negligible;
- the engine intake, compressor, turbine and propelling nozzle are described by means of the following polytropic efficiencies, which can be considered as representative of current technology [4]:

$$\eta_{p,i} = 0.95;\ \eta_{p,c} = 0.89;\ \eta_{p,t} = 0.8;\ \eta_{p,n} = 0.91$$

Figure 7 shows the different cycle points considered for the proposed analysis. T_{3co} denotes the temperature that the combustion gases would achieve if the fuel heating value is completely released as heat (i.e., complete oxidation of the fuel). T_{3co} is thus the adiabatic flame temperature used for simplified cycle analysis calculations. Point 3 refers to the combustor outlet.

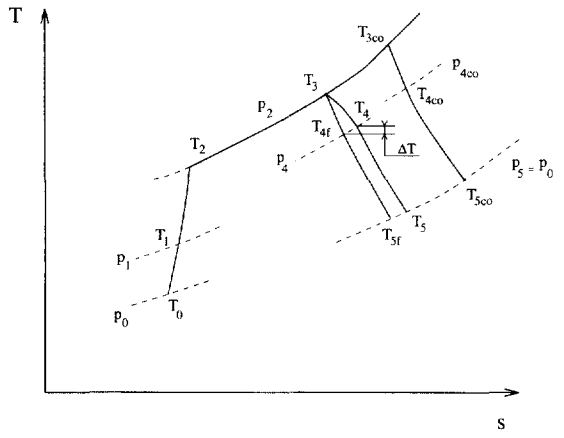

Figure 7. Thermodynamic cycle of jet-engine.

Assuming that the average fluid specific heats for transformations 2–3 and 2–3co are essentially identical, temperatures T_3 and T_{3co} are related by the chemical heat release efficiency, defined by equation (7) and evaluated at the combustor exit (point 3):

$$\eta_{chr,3} = \frac{h_3 - h_2}{h_{3co} - h_2} = \frac{T_3 - T_2}{T_{3co} - T_2} \tag{8}$$

For cycle 0–2–3co–4co–5co, point 4co is computed such that the work required to drive the compressor is exactly matched by the turbine work output.

Point 4 is computed assuming chemically reactive flow in the turbine, whereas point 4f results from assuming chemically inert behavior of the gas which is expanded to the same pressure as that considered for point 4. Temperature T_4 is obtained from temperature T_{4f} by adding the temperature difference ΔT computed with the one-dimensional flow model presented in the previous sections. Indeed ΔT represents the temperature difference at the turbine outlet between a reacting and a non reacting fluid frictionless expansion from temperature T_3 and pressure p_2 to pressure p_4, whereas $T_4 - T_{4f}$ represents the temperature difference between a reacting and a non reacting fluid polytropic expansion from temperature T_3 and pressure p_2 to pressure p_4. Because of the low relative importance of the frictions it is actually acceptable to assume that these two temperature differences are equal. This assumption is further justified by the low numerical value of ΔT compared to the other temperature differences appearing in equations (8) to (15).

Pressure p_4 is such that the compressor work requirements are matched by the turbine. Based on the hypotheses adopted for this study, this leads directly to the following relationships:

$$T_3 - T_4 + \Delta T = T_3 - T_{4f} = T_{3co} - T_{4co} = T_2 - T_1 \tag{9}$$

In the same way, we have the following relation for thermal efficiencies at sea-level static conditions:

$$\frac{\eta_{th}}{\eta_{thco}} = \frac{T_4 - T_5}{T_{4co} - T_{5co}} \tag{10}$$

Observation of the temperature differences in the thermodynamic cycle diagram (*figure 7*) as well as numerical simulation results lead to the following conclusion:

$$\frac{\eta_{th}}{\eta_{thco}} < \eta_{chr,3} \tag{11}$$

From the thermodynamic point of view this means that the penalty due to operating the engine at a temperature T_3 far smaller than the adiabatic flame temperature T_{3co} is more severe than the gain obtained from expanding the gas with a heat release q instead of expanding it adiabatically.

The *specific thrust* F is simply defined by:

$$F = w_5 - v_0 \tag{12}$$

The overall efficiency η_o defined as the product of thermal efficiency η_{th} and propulsion efficiency η_{pro} may be written as follows:

$$\begin{cases} \eta_{pro} = \dfrac{2\,v_0}{w_5 + v_0} \\ \\ \eta_{th} = \dfrac{\dot{m}\,(w_5^2 - v_0^2)}{2\,\dot{Q}} \end{cases} \Rightarrow \eta_o = \frac{\dot{m}\,v_0\,(w_5 - v_0)}{\dot{Q}} \tag{13}$$

Note that at sea-level static conditions, we take $\eta_o = \eta_{th}$ since $\eta_{pro} = 0$. v_0 represents the cruise velocity and w_5 the relative speed of the gases ejected from the nozzle. The latter can be computed as follows:

$$w_5 = \sqrt{2\,c_p\,(T_4 - T_5)} \tag{14}$$

for the reactive flow case and:

$$w_5 = \sqrt{2\,c_p\,(T_{4co} - T_{5co})} \tag{15}$$

assuming complete oxidation of the fuel.

$\dot{Q}$ is the heat supplied to the jet-engine and is computed as follows:

$$\dot{Q} = \dot{m}_{C_{12}H_{26}}\,LHV_{C_{12}H_{26}} \tag{16}$$

5. RESULTS OF THE ENGINE PERFORMANCE ANALYSIS

Figure 8 shows the variations of the temperature difference $T_{3co} - T_3$ as a function of compression ratio for the different flight conditions considered in this paper. We note that the difference between T_{3co} and T_3 is considerable, particularly at high temperature and low compression ratios.

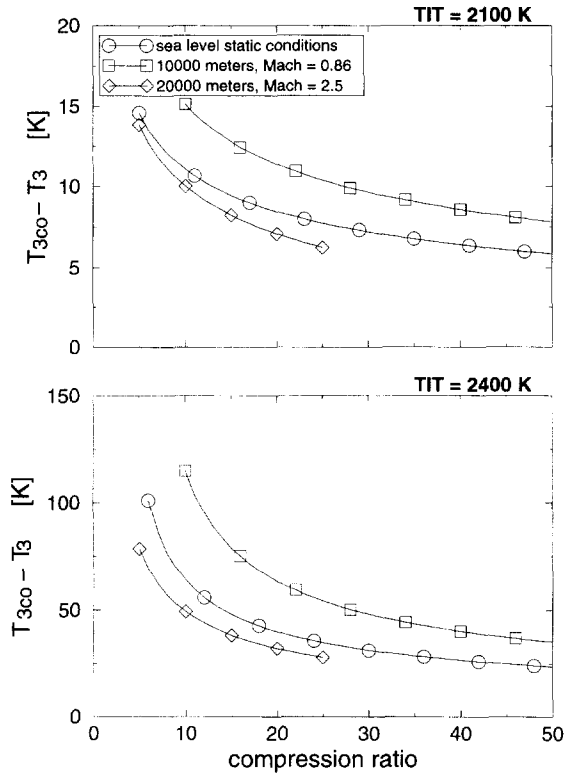

Figure 8. $(T_{3co} - T_3)$ vs. compression ratio.

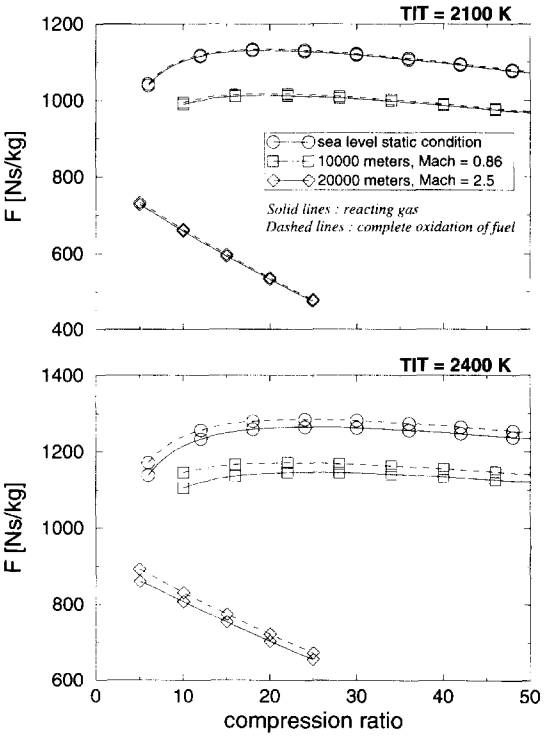

Figure 9. Specific thrust F vs. compression ratio.

Figure 9 shows profiles of the specific thrust F. We note that the specific thrust is maximum at sea-level static conditions and decreases with altitude and flight speed. At $TIT = 2\,400$ K we observe a marked difference between the two cases considered. The chemical reactivity of the expanding gas stream results in a significant decrease of thrust. This effect is more pronounced for low compression ratios.

Figure 10 shows the overall efficiency plotted versus compression ratio. The low overall efficiencies obtained for commercial aviation flight conditions (i.e., 10 000 m altitude, $Mach = 0.86$) are a well known result. We recall that this paper considers only the simple turbo-jet engine. For commercial aviation conditions, significantly better results are obtained by adopting the more sophisticated turbo-fan cycle, which is not considered here.

The key result in *figure 10* is that in flight conditions, the increase of operating temperature *decreases* the overall efficiency. Moreover, at high temperatures the gas chemical reactivity causes a marked decrease of the overall efficiency. At $TIT = 2\,400$ K, a difference of more than 2 percentage points can be observed at sea-level static conditions for high compression ratios. *Figure 11* presents the same results for the particular case of sea-level static operation with low compression ratios.

We again note that for compression ratios lower than 17, the effect of chemical reactivity of the expanding combustion gases is to *decrease* the efficiency when the temperature is increased.

6. CONCLUSIONS

The results presented in this paper suggest that, for current high temperature turbo-jet engines (i.e. TITs on the order of 2 100 K), chemical reactivity of the expanding gas stream has little impact on engine performance. However, given the current trend towards even higher TITs, the results show that chemical reactivity may have a significant effect on the performance and environmental characteristics of future jet-engines. In particular, we may note the following.

1) At ultra-high temperatures, pollutant production in the combustion chamber is significant. Chemical reactivity of the hot gas stream in the turbine leads to further NO production in the turbine. Conversely, CO partially recombines with oxygen, resulting in a decrease of CO composition within the stage. Heat is released due to this recombination process, which modifies the flow characteristics of the expanding gas stream. However, η_{chr} is well below 100 % at the turbine inlet, and only

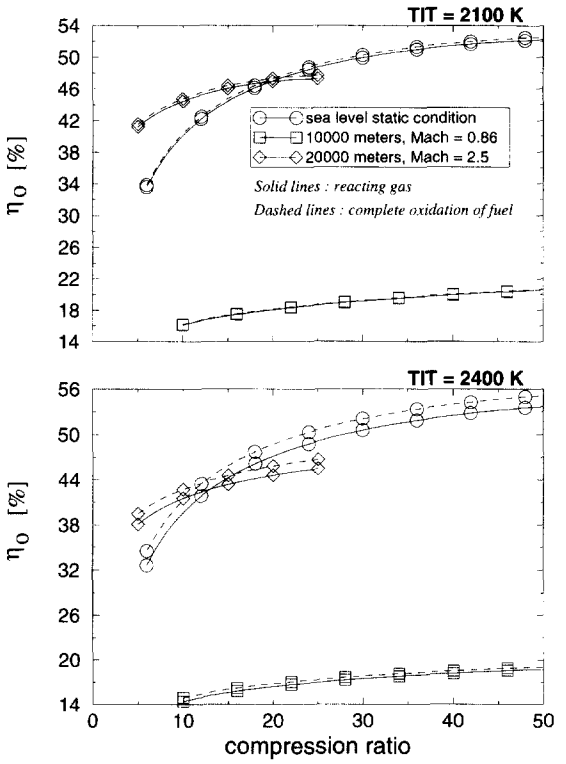

Figure 10. Overall efficiency η_0 vs. compression ratio.

part of the heat unreleased in the combustor is recovered in the turbine as a result of chemical reactivity. Thus, for high TIT engines, overall efficiency and specific thrust are lower than the values computed assuming full release of the fuel heating value in the combustor.

2) The production of environmental pollutants in the turbine as a result of chemical reactivity is particularly significant for turbo-jets operating at subsonic cruise velocities.

3) At take-off, the amount of heat released by chemical reactions in the turbine stage is over 2.5 % of the enthalpy drop in the turbine, for a high TIT (2 400 K) engine.

4) For low compression ratios and high TIT levels, an increase of TIT leads to a *decrease* of thermal efficiency at sea-level static condition.

5) In flight conditions, the increase of operating temperature *decreases* the overall efficiency.

This study therefore questions the current trend which consists in increasing firing temperature to increase performance. At high temperature levels, the effects of chemical reactivity of the expanding hot gases lead to unacceptable pollutant emission levels and tend to counteract any potential gain in efficiency suggested by a study considering complete oxidation of the fuel.

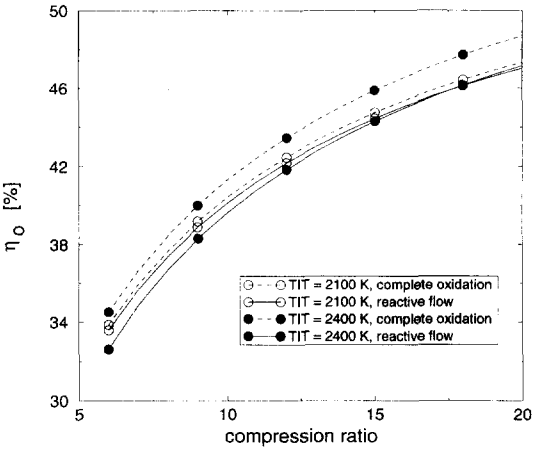

Figure 11. Overall (thermal) efficiency η_0 vs. compression ratio at sea-level static conditions.

REFERENCES

[1] Clouser S.D., Kamin R.A., Combustion technology needs for advanced high pressure cycle engines, in: AGARD meeting on Fuels and Combustion Technology for Advanced Aircraft Engines, May 1993.

[2] De Piolenc M., Latest jet engine technology could radically change industrial designs, Gas Turbine World 22 (5) (1992) 46–50.

[3] Godin T., Harvey S., Stouffs P., High-temperature reactive flow of combustion gases in an expansion turbine, J. Turbomachinery–T. ASME 119 (1997) 554–561.

[4] Godin T., Harvey S., Stouffs P., Chemically reactive flow of hot combustion gases in an aircraft turbo-jet engine, in: Proceedings of the International Gas Turbine and Aeroengine Congress and Exhibition, ASME, 97-GT-302, 1997.

[5] Cohen H., Rogers G.F.C., Saravanamutoo H.I.H., Gas Turbine Theory, 3rd ed., Longman Scientific & Technical, John Wiley & Sons, New York, 1987.

[6] Leide B., Stouffs P., Residual reactivity of burned gases in the early expansion process of future gas turbines, J. Eng Gas Turb Power, 118 (1996) 54–60.

[7] Hoffman J.D., Zucrow M.J., Gas Dynamics 2, John Wiley & Sons, New York, 1977.

[8] Reynolds W.C., A Fortran package for the analysis of gas phase chemical equilibriums, Stanford University, version 3.8C, 1988.

[9] Lefebvre A.H., Gas turbine combustion, Hemisphere Publ. Corp., New York, 1983.

[10] Miller J.A., Bowman C.T., Mechanism and modeling of nitrogen chemistry in combustion, Prog. Energ. Combust. 15 (1989) 287–338.

[11] Harvey S., Étude du mécanisme réactionnel régissant la détente chimiquement réactive des produits de combustion dans une turbine à gaz, Internal Report, Isitem Nantes, 1995.

[12] Kee R.J., Rupley R.F., Miller J.A., A Fortran chemical kinetics package for the analysis of gas phase chemical kinetics, SANDIA Report SAND89-8009B, 1989.

[13] Godin T., Activité chimique des gaz de combustion au cours de la détente dans les futures turbines à gaz, Thèse, École des Mines de Paris, 1996.